

Precise Measurement of the Form Factors in $D^0 \rightarrow K^*(892)^-\mu^+\nu_\mu$, and Test of Lepton Universality with $D^0 \rightarrow K^*(892)^-\ell^+\nu_\ell$ Decays

M. Ablikim *et al.**
(BESIII Collaboration)

 (Received 15 April 2025; revised 3 June 2025; accepted 19 August 2025; published 10 September 2025)

We report a study of the semileptonic decay $D^0 \rightarrow \bar{K}^0\pi^-\mu^+\nu_\mu$ based on a sample of 7.9 fb^{-1} of e^+e^- annihilation data collected at a center-of-mass energy of 3.773 GeV with the BESIII detector at the BEPCII collider. The branching fraction of the decay is measured for the first time to be $\mathcal{B}(D^0 \rightarrow \bar{K}^0\pi^-\mu^+\nu_\mu) = (1.373 \pm 0.020_{\text{stat}} \pm 0.023_{\text{syst}})\%$, where the first uncertainty is statistical and the second is systematic. Based on the investigation of the decay dynamics, we find that the decay is dominated by the $K^*(892)^-$ resonance with the branching fraction measured to be $\mathcal{B}(D^0 \rightarrow K^*(892)^-\mu^+\nu_\mu) = (1.948 \pm 0.033_{\text{stat}} \pm 0.036_{\text{syst}})\%$. We also determine the hadronic form factors for the $D^0 \rightarrow K^*(892)^-\mu^+\nu_\mu$ decay to be $r_V = V(0)/A_1(0) = 1.46 \pm 0.11_{\text{stat}} \pm 0.04_{\text{syst}}$, $r_2 = A_2(0)/A_1(0) = 0.71 \pm 0.08_{\text{stat}} \pm 0.03_{\text{syst}}$, and $A_1(0) = 0.609 \pm 0.008_{\text{stat}} \pm 0.008_{\text{syst}}$, where $V(0)$ is the vector form factor and $A_{1,2}(0)$ are the axial-vector form factors evaluated at $q^2 = 0$. The $A_1(0)$ is measured for the first time in $D^0 \rightarrow K^*(892)^-\mu^+\nu_\mu$ decay. Averaging the form factor parameters that we reported previously in $D^0 \rightarrow K^*(892)^-(\rightarrow \bar{K}^0\pi^-)e^+\nu_e$ and $D^0 \rightarrow K^*(892)^-(\rightarrow K^-\pi^0)\mu^+\nu_\mu$ decays, we obtain $r_V = 1.456 \pm 0.040_{\text{stat}} \pm 0.016_{\text{syst}}$, $r_2 = 0.715 \pm 0.031_{\text{stat}} \pm 0.014_{\text{stat}}$, and $A_1(0) = 0.614 \pm 0.005_{\text{stat}} \pm 0.004_{\text{syst}}$. This is the most precise determination of the form factor parameters to date measured in $D \rightarrow K^*(892)$ transitions, which provide the most stringent test on various theoretical models.

DOI: [10.1103/zfxr-dlzg](https://doi.org/10.1103/zfxr-dlzg)

Semileptonic (SL) decays of D mesons provide valuable information on the weak and strong interactions within hadrons composed of heavy quarks [1,2]. The partial decay rate is related to the product of the hadronic form factor (FF) describing the effects of the strong interaction in the initial and final hadrons, and the Cabibbo-Kobayashi-Maskawa (CKM) matrix [3] element $|V_{cs(d)}|$ parametrizing the mixing of quarks in the weak interaction. Because of $|V_{cs(d)}|$ being tightly constrained by CKM unitarity, studies of D meson SL decays provide an ideal laboratory to extract these hadronic FFs. In recent years, there has been an accumulation of hadronic FF measurements in $D \rightarrow V\ell^+\nu_\ell$ decays [4–15], where V and ℓ refer to a vector meson and a lepton, respectively. Furthermore, the SL decay $D^0 \rightarrow K^*(892)^-\ell^+\nu_\ell$ also plays a crucial role in understanding the standard model (SM), as it provides the most direct way to experimentally extract the value of $|V_{cs}|$. However, such an extraction requires precise theoretical

knowledge of the hadronic FFs taking into account non-perturbative quantum chromodynamic (QCD) effects.

In theory, although the study of the $D \rightarrow K^*(892)$ transition is very challenging, calculations are extensively carried out by a series of nonperturbative approaches including lattice QCD [16], light cone sum rules (LCSR) [17,18], the constituent quark model (CQM) [19,20], heavy quark effective theory (HQEFT) [21], the combined heavy meson and chiral theory (HM χ T) [22], the covariant light-front quark model (CLFQM) [23,24], the large energy chiral quark model (LE χ QM) [25], the covariant confined quark model (CCQM) [26], the relativistic quark model (RQM) [27], and holographic QCD [28]. In these theoretical calculations, one vector FF $V(q^2)$ and two axial-vector FFs $A_{1,2}(q^2)$, are introduced to describe the effects of the strong interactions. However, the FF parameters of $r_V = V(0)/A_1(0)$, $r_2 = A_2(0)/A_1(0)$, and $A_1(0)$ in the $D \rightarrow K^*(892)$ transition predicted by these models [16–28] differ significantly and vary in the ranges from 1.36–1.60, 0.50–0.92, and 0.57–0.66, respectively. Currently, the precision in measuring r_V and r_2 is still poor [29], and no direct measurement of $A_1(0)$ is available in $D^0 \rightarrow K^*(892)^-\mu^+\nu_\mu$ decay [29]. Therefore, precise measurements of these FF parameters can provide stringent tests and rigorous calibrations on various nonperturbative calculations. Furthermore, these data also represent a

*Full author list given at the end of the Letter.

Published by the American Physical Society under the terms of the [Creative Commons Attribution 4.0 International license](https://creativecommons.org/licenses/by/4.0/). Further distribution of this work must maintain attribution to the author(s) and the published article's title, journal citation, and DOI. Funded by SCOAP³.

valuable motivation for updating lattice QCD calculations [16].

In the SM, the SL decays of D mesons offer an excellent opportunity to test lepton flavor universality (LFU) [30,31]. In Refs. [18,20,32,33], it is suggested that observable LFU violation effects may occur in SL decays via $c \rightarrow s\ell^+\nu_\ell$. In particular, the multiple polarization states of vector mesons in $D \rightarrow V\ell^+\nu_\ell$ decay provide more physical information, allowing a more detailed search for potential new physics effects. In recent years, the branching fraction (BF) of $D^0 \rightarrow K^*(892)^-\mu^+\nu_\mu$ and the ratio $R_{K^*(892)}^{\mu/e} = \{\mathcal{B}[D^0 \rightarrow K^*(892)^-\mu^+\nu_\mu]/\mathcal{B}[D^0 \rightarrow K^*(892)^-e^+\nu_e]\}$ have been calculated using various theoretical models, leading to differing expectations. The predicted BF within the SM framework varies by (1.82–3.09)% [17–27], and $R_{K^*(892)}^{\mu/e}$ is found to be between 0.92–0.95 in Refs. [17,20,24–27,34] and 0.99 in Ref. [18]. Furthermore, the ratio of the decay rates ($R_{L/T}$) between the longitudinally and transversely polarized K^* fractions in the $D^0 \rightarrow K^*(892)^-\mu^+\nu_\mu$ decay is predicted to be sensitive to the pseudoscalar Wilson coefficient $c_p^{(\ell)}$ [33], while no corresponding measurement has been reported yet [29].

The SL decay $D^0 \rightarrow \bar{K}^0\pi^-\mu^+\nu_\mu$ was first measured by the FOCUS collaboration [10], where only the FF ratios r_V and r_2 were reported with limited precision. No other measurements have been performed in the last two decades. In this Letter, we report the first measurement of the absolute BF for $D^0 \rightarrow \bar{K}^0\pi^-\mu^+\nu_\mu$, and the most precise measurements of FF parameters r_V , r_2 , and $A_1(0)$ in the decay $D^0 \rightarrow K^*(892)^-\ell^+\nu_\ell$. Throughout this Letter, charge-conjugate modes are implied unless explicitly noted. These measurements are performed using a data sample corresponding to an integrated luminosity of 7.9 fb^{-1} produced at the center-of-mass energy $\sqrt{s} = 3.773 \text{ GeV}$ with the BEPCII e^+e^- collider and collected by the BESIII detector [35].

Simulated data samples produced with a Geant4-based Monte Carlo (MC) package [36], which includes the geometric description of the BESIII detector and the detector response, are used to determine detection efficiencies and to estimate background contributions. The simulation models the beam energy spread and initial state radiation (ISR) in the e^+e^- annihilations with the KKMC generator [37]. The inclusive MC sample includes the production of $D\bar{D}$ pairs, the non- $D\bar{D}$ decays of the $\psi(3770)$, the ISR production of the J/ψ and $\psi(3686)$ states, and the continuum processes incorporated in KKMC [37]. All particle decays are modeled with EvtGen [38] using branching fractions either taken from the Particle Data Group [29], when available, or otherwise estimated with LUNDCHARM [39]. Final state radiation (FSR) from charged final state particles is incorporated using the PHOTOS package [40]. The generation of the signal

TABLE I. The selection requirements on ΔE , the ST yields N_{ST} in data, the ST and DT efficiencies, ϵ_{ST} and ϵ_{DT} , for each of the six tag decay modes. For ϵ_{DT} , the BF of $\bar{K}^0 \rightarrow \pi^+\pi^-$ is not included.

ST mode	ΔE (GeV)	$N_{\text{ST}}^i (\times 10^3)$	ϵ_{ST}^i (%)	ϵ_{DT}^i (%)
$K^+\pi^-$	[−0.027, 0.027]	1449.3 ± 1.3	65.34(01)	13.88(02)
$K^+\pi^-\pi^-\pi^+$	[−0.026, 0.024]	1944.2 ± 1.6	40.83(01)	6.96(02)
$K^+\pi^-\pi^0$	[−0.062, 0.049]	2913.2 ± 2.0	35.59(01)	7.15(02)
$K_S^0\pi^+\pi^-$	[−0.024, 0.024]	447.6 ± 0.7	37.49(01)	6.05(02)
$K^+\pi^-\pi^0\pi^0$	[−0.068, 0.053]	690.6 ± 1.3	14.83(01)	2.89(01)
$K^+\pi^-\pi^+\pi^-\pi^0$	[−0.057, 0.051]	450.9 ± 1.1	16.17(01)	2.40(01)

$D^0 \rightarrow \bar{K}^0\pi^-\mu^+\nu_\mu$ incorporates knowledge of the FFs obtained in this Letter.

Our analysis makes use of both “single-tag” (ST) and “double-tag” (DT) samples of D decays. The ST samples are \bar{D}^0 events reconstructed from one of their six hadronic decays as listed in Table I, while the DT samples are events with a ST and a D^0 meson reconstructed as $D^0 \rightarrow \bar{K}^0\pi^-\mu^+\nu_\mu$. The BF for the SL decay is given by [12]

$$\mathcal{B}_{\text{SL}} = \frac{N_{\text{DT}}}{\sum_i N_{\text{ST}}^i (\epsilon_{\text{DT}}^i / \epsilon_{\text{ST}}^i)} = \frac{N_{\text{DT}}}{N_{\text{ST}} \epsilon_{\text{SL}}}, \quad (1)$$

where $N_{\text{DT(ST)}}$ is the total yield of DT(ST) events, $\epsilon_{\text{SL}} = (\sum_i N_{\text{ST}}^i \times \epsilon_{\text{DT}}^i / \epsilon_{\text{ST}}^i) / \sum_i N_{\text{ST}}^i$ is the average efficiency of reconstructing the SL decay in a ST event, weighted by the measured yields of ST modes in the data, and ϵ_{ST}^i and ϵ_{DT}^i are the efficiencies for finding the ST and the SL decay in the i th tag mode, respectively.

A detailed description of the selection criteria for π^\pm , K^\pm , γ , π^0 , K_S^0 , and π^0 candidates is given in Ref. [12]. The ST \bar{D}^0 mesons are identified using the beam constrained mass:

$$M_{\text{BC}} = \sqrt{(\sqrt{s}/2)^2 - |\vec{p}_{\bar{D}^0}|^2}, \quad (2)$$

where $\vec{p}_{\bar{D}^0}$ is the momentum of the \bar{D}^0 candidate in the rest frame of the initial e^+e^- system. A kinematic variable $\Delta E = E_{\bar{D}^0} - \sqrt{s}/2$ for each candidate is used to improve the signal significance for ST \bar{D}^0 mesons, where $E_{\bar{D}^0}$ is the energy of the \bar{D}^0 candidate. The explicit ΔE requirements for these six ST modes are listed in Table I. The distributions of the variable M_{BC} for the six ST modes are shown in Fig. 1, where maximum likelihood fits to the M_{BC} distributions are performed. The signal function is derived from the convolution of the MC-simulated signal shape with a double-Gaussian function to account for resolution difference between simulation and data, where the parameters of the double-Gaussian function are floated. An ARGUS function [41] is used to describe the combinatorial background shape. For each tag mode, the ST yield is

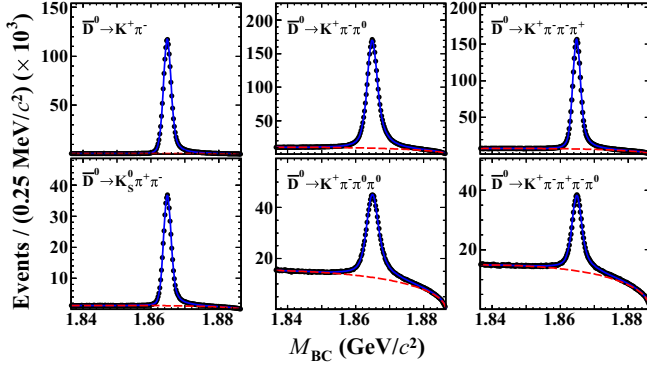


FIG. 1. The M_{BC} distributions of the six ST modes. The points are data, the solid blue curves are the projection of the sum of all fit components, and the dashed red curves are the projection of the background component of the fit.

obtained by integrating the signal function over the D^0 signal region within $1.859 < M_{BC} < 1.873$ GeV/c^2 . The ST yields and the ST efficiencies for six ST modes are listed in Table I. The total ST yield summed over all six ST modes is $N_{\text{ST}} = (7895.8 \pm 3.4) \times 10^3$, where the uncertainty is statistical only.

Candidates for the SL decay $D^0 \rightarrow \bar{K}^0 \pi^- \mu^+ \nu_\mu$ are selected from the remaining tracks recoiling against the ST \bar{D}^0 mesons. The \bar{K}^0 meson is reconstructed as a $K_S^0 \rightarrow \pi^+ \pi^-$ decay with the same selection criteria used in the ST side. In addition to the two charged tracks originating from K_S^0 decays, the event must contain exactly two additional tracks with opposite charges. The track having the same charge of the kaon on the tagging side is taken as the muon candidate. For muon particle identification (PID), the dE/dx and time-of-flight system (TOF) measurements are combined with shower properties from the electromagnetic calorimeter (EMC) to construct likelihoods for electron, muon, pion, and kaon hypotheses, \mathcal{L}_e , \mathcal{L}_μ , \mathcal{L}_π , and \mathcal{L}_K . The muon candidate must satisfy $\mathcal{L}_\mu > 0.001$, $\mathcal{L}_\mu > \mathcal{L}_e$, $\mathcal{L}_\mu > \mathcal{L}_K$, and $\mathcal{L}_\mu / (\mathcal{L}_\mu + \mathcal{L}_\pi + \mathcal{L}_K) > 0.3$. Additionally, the deposited EMC energy of the muon candidate (EMC_μ) should be within $0.1 < \text{EMC}_\mu < 0.3$ GeV. The other charged track is taken as the pion candidate and must satisfy $\mathcal{L}'_\pi > \mathcal{L}'_K$, where \mathcal{L}'_π and \mathcal{L}'_K are PID likelihoods calculated with dE/dx and TOF measurements for the pion and kaon hypotheses, respectively. For the ST mode $K_S^0 \pi^+ \pi^-$, it is possible that two combinations are selected for the muon and pion candidates. Only the combination with the maximum product likelihoods $\mathcal{L}_\mu \mathcal{L}'_\pi$ is retained. The background candidates from $D^0 \rightarrow \bar{K}^0 \pi^+ \pi^- (\pi^0)$ decays reconstructed as $D^0 \rightarrow \bar{K}^0 \pi^- \mu^+ \nu_\mu$ are rejected by requiring the $\bar{K}^0 \pi^- \mu^+ (\pi^0)$ invariant mass ($M_{\bar{K}^0 \pi^- \mu^+ (\pi^0)}$) to be less than 1.60 GeV/c^2 , where the π^0 is reconstructed with the residual photon pairs in the signal side. Background events

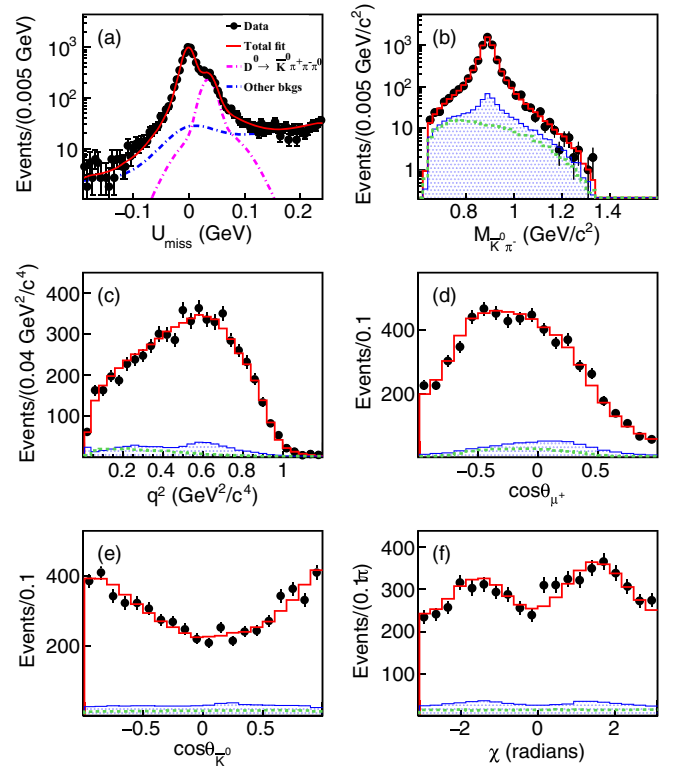


FIG. 2. (a) Fit of the SL candidate events to the U_{miss} distribution. Distributions of the five kinematic variables (b) $M_{\bar{K}^0 \pi^-}$, (c) q^2 , (d) $\cos \theta_{\mu^+}$, (e) $\cos \theta_{\bar{K}^0}$, and (f) χ for the SL decay $D^0 \rightarrow \bar{K}^0 \pi^- \mu^+ \nu_\mu$, where the green dashed curves show the contribution of the \mathcal{S} -wave component. In these plots, the dots with error bars are data, the red curve or histograms are the fit results, and the shaded histograms are the simulated background.

containing additional π^0 mesons are further suppressed by requiring the maximum energy of any unused photon ($E_{\gamma \text{max}}$) to be less than 0.15 GeV.

As the neutrino is not detected, we employ the kinematic variable $U_{\text{miss}} = E_{\text{miss}} - c|\vec{p}_{\text{miss}}|$ to obtain information on the neutrino, where E_{miss} and \vec{p}_{miss} are the missing energy and momentum carried by the neutrino, respectively, and are defined in the same way as in Ref. [12]. Figure 2(a) shows the U_{miss} distribution of the accepted candidates for $D^0 \rightarrow \bar{K}^0 \pi^- \mu^+ \nu_\mu$ in data. To obtain the signal yield, an unbinned maximum likelihood fit to the U_{miss} distribution is performed. In the fit, the signal is described with a shape derived from the simulated signal events convolved with a Gaussian function, where the mean and width of the Gaussian function are determined by the fit. The peaking background from $D^0 \rightarrow \bar{K}^0 \pi^- \pi^+ \pi^0$ is modeled using the MC-derived shape. The other combinatorial background contribution is described using the shape obtained from the inclusive MC simulation. The yield of $D^0 \rightarrow \bar{K}^0 \pi^- \mu^+ \nu_\mu$ events is $N_{\text{DT}} = 6796 \pm 98$, where the uncertainty is statistical only.

The DT efficiency ϵ_{DT}^i for each tag mode is summarized in the last column of Table I, and the average efficiency of

reconstructing SL decay, ϵ_{SL} , is estimated to be $(18.98 \pm 0.01)\%$. The difference of the K_S^0 reconstruction efficiencies between data and MC is estimated to be $-(1.8 \pm 0.6)\%$, taking into account the systematic uncertainties due to the tracking efficiencies for the charged pions, the K_S^0 mass window, and decay length requirements. The difference due to the μ PID efficiency between data and MC is estimated to be $-(2.8 \pm 0.4)\%$ evaluated using the control sample of $e^+e^- \rightarrow \gamma\mu^+\mu^-$ decay. Hence, ϵ_{SL} is further corrected by -1.8% and -2.8% , giving $(18.12 \pm 0.01)\%$ [42]. The BF of the decay is measured to be $\mathcal{B}(D^0 \rightarrow \bar{K}^0\pi^-\mu^+\nu_\mu) = (1.373 \pm 0.020_{\text{stat}})\%$.

Because of the DT technique, the BF measurement is insensitive to the systematic uncertainty in the ST efficiency. The uncertainty on the muon tracking (PID) efficiency is estimated to be 0.3% (0.4%) by studying a sample of $e^+e^- \rightarrow \gamma\mu^+\mu^-$ events. The uncertainty due to the pion tracking (PID) efficiency is estimated to be 0.3% (0.3%) using control samples selected from $D^0 \rightarrow K^-\pi^+(\pi^0, \pi^+\pi^-)$ and $D^+ \rightarrow K^-\pi^+\pi^+(\pi^0)$. The uncertainty from K_S^0 reconstruction is 0.6% , determined with control samples selected from $D^0 \rightarrow \bar{K}^0\pi^+\pi^-$, $\bar{K}^0\pi^+\pi^-\pi^0$, $\bar{K}^0\pi^0$, and $D^+ \rightarrow \bar{K}^0\pi^+$, $\bar{K}^0\pi^+\pi^0$, $\bar{K}^0\pi^+\pi^+\pi^-$. The uncertainty associated with the $E_{\gamma\text{max}}$ requirement is estimated to be 0.7% by analyzing DT $D^0\bar{D}^0$ events where D^0 mesons decay to hadronic final states of $D^0 \rightarrow K^-\pi^+$, $K^-\pi^+\pi^0$, and $K^-\pi^+\pi^+\pi^-$. The uncertainty due to the $M_{\bar{K}^0\pi^-\mu^+(\pi^0)}$ requirement is estimated to be 0.9% evaluated using a control sample from $D^+ \rightarrow K^-\pi^+e^+\nu_e$ with the positron mass substituted by the μ mass. The uncertainty due to the modeling of the signal in simulated events is estimated to be 0.7% by varying the input FF parameters determined in this Letter by $\pm 1\sigma$. The uncertainty associated with the fit to the U_{miss} distribution is estimated to be 0.6% by varying the fitting ranges and the shapes, which parametrize the signal and background candidates, where an asymmetric Gaussian function is used as an alternative signal function. The uncertainty associated with the fit of the M_{BC} distributions used to determine N_{ST} is 0.1% and is evaluated by varying the bin size, fit range, and background distributions. Further systematic uncertainties are assigned due to the statistical precision of the simulation, 0.3% , and the input BF of the decay $K_S^0 \rightarrow \pi^+\pi^-$, 0.1% . The systematic uncertainty contributions are summed in quadrature, and the total systematic uncertainty on the BF measurement is 1.7% . Finally, we obtain $\mathcal{B}(D^0 \rightarrow \bar{K}^0\pi^-\mu^+\nu_\mu) = (1.373 \pm 0.020_{\text{stat}} \pm 0.023_{\text{sys}})\%$.

The differential decay rate of $D^0 \rightarrow \bar{K}^0\pi^-\mu^+\nu_\mu$ can be expressed in terms of five kinematic variables: the squared invariant mass of the $\bar{K}^0\pi^-$ system ($m_{\bar{K}^0\pi^-}^2$), the squared transfer momentum of μ^+ and ν_μ (q^2), the angle between π^- and the D^0 direction in the $\bar{K}^0\pi^-$ rest frame ($\theta_{\bar{K}^0}$), the angle between ν_μ and the D^0 direction in the $\mu^+\nu_\mu$ rest frame (θ_μ), and the acoplanarity angle (χ) between the two decay

planes of $\bar{K}^0\pi^-$ and $\mu^+\nu_\mu$. The differential decay rate is expressed as [43,44]

$$d^5\Gamma = \frac{G_F^2 |V_{cs}|^2}{(4\pi)^6 m_{D^0}^3} X\beta\beta_\mu \mathcal{I}(m_{\bar{K}^0\pi^-}^2, q^2, \theta_{\bar{K}^0}, \theta_\mu, \chi) \times dm_{\bar{K}^0\pi^-}^2 dq^2 d\cos\theta_{\bar{K}^0} d\cos\theta_\mu d\chi, \quad (3)$$

where $X = p_{\bar{K}^0\pi^-} m_{D^0}$, $\beta = 2p^*/m_{\bar{K}^0\pi^-}$, $\beta_\mu = (1 - m_\mu^2/q^2)$. Furthermore, $p_{\bar{K}^0\pi^-}$ is the momentum of the $\bar{K}^0\pi^-$ system in the D^0 rest frame, p^* is the momentum of \bar{K}^0 in the $\bar{K}^0\pi^-$ rest frame, m_μ (m_{D^0}) is the known μ (D^0) mass [29], and G_F is the Fermi coupling constant. The detailed expression of \mathcal{I} is documented in Supplemental Material [45].

To extract the FF parameters, an unbinned five-dimensional maximum likelihood fit to the distributions of $m_{\bar{K}^0\pi^-}$, q^2 , $\cos\theta_{\bar{K}^0}$, $\cos\theta_\mu$, and χ for the signal candidates within $-0.02 < U_{\text{miss}} < 0.02$ GeV is performed in the same manner as in Ref. [12]. The parameterization of the \mathcal{S} -wave phase takes the form of $\delta_S(m) = \delta_{\text{BG}}^{1/2}$ [12]. In the fit, the FF ratios r_V and r_2 , the mass $M_{K^*(892)^-}$ and width $\Gamma_{K^*(892)^-}$, the relative intensity r_S , scattering length $a_{\text{S,BG}}^{1/2}$, and the dimensionless coefficient $r_S^{(1)}$ are set to be free variables, while the effective range $b_{\text{S,BG}}^{1/2}$ is fixed to -0.81 (GeV/c) $^{-1}$, taken from Ref. [9]. The projected distributions of the fit onto the fitted variables are shown in Figs. 2(b)–2(f). The fit results are summarized in Table II. The goodness of the fit is estimated as in Ref. [12] and χ^2/ndof is evaluated to be $115.9/101$.

The fit fraction of each component can be determined by the ratio of the decay intensity of the specific component to that of the total intensity. The fractions of \mathcal{S} wave and \mathcal{P} wave [$K^*(892)^-$] are $f_{\mathcal{S}\text{wave}} = (5.35 \pm 0.87_{\text{stat}})\%$ and $f_{K^*(892)^-} = (94.60 \pm 0.87_{\text{stat}})\%$, respectively, where the uncertainty propagation includes correlations among the underlying parameters. The systematic uncertainties of the fit parameters and the fractions of \mathcal{S} -wave and $K^*(892)^-$ components are defined as the difference between the nominal fit and the alternative fits with varied conditions. The systematic uncertainties due to the requirements on $E_{\gamma\text{max}}$, $M_{\bar{K}^0\pi^-\mu^+(\pi^0)}$, μ_{PID} , background subtraction, tracking and PID, the possible \mathcal{D} -wave component, and the fixed $b_{\text{S,BG}}^{1/2}$ are evaluated in the same way as in Ref. [12]. The systematic uncertainty for each source is documented in Supplemental Material [45]. The total absolute systematic uncertainty for each fit parameter is also listed in Table II.

The value of $A_1(0)$ is obtained by integrating Eq. (3), restricted to the $K^*(892)^-$ contribution, over the three angles:

TABLE II. The fit results, where the first uncertainty is statistical and the second is systematic.

Variable	Value
$M_{K^*(892)^-}$ (MeV/c ²)	$892.7 \pm 0.5 \pm 0.1$
$\Gamma_{K^*(892)^-}$ (MeV)	$45.6 \pm 0.8 \pm 0.1$
r_S (GeV) ⁻¹	$-12.44 \pm 2.40 \pm 3.04$
$d_{S,BG}^{1/2}$ (GeV/c) ⁻¹	$3.33 \pm 0.53 \pm 1.06$
$r_S^{(1)}$	$0.06 \pm 0.20 \pm 0.26$
r_V	$1.46 \pm 0.11 \pm 0.04$
r_2	$0.71 \pm 0.08 \pm 0.03$

$$\frac{d^2\Gamma}{dq^2 dm_{\bar{K}^0\pi^-}^2} = \frac{2X_\mu G_F^2 |V_{cs}|^2}{9 (4\pi)^5 m_{D^0}^2} P_{\bar{K}^0\pi^-} \times \beta(|\mathcal{F}_{11}|^2 + |\mathcal{F}_{21}|^2 + |\mathcal{F}_{31}|^2), \quad (4)$$

where $X_\mu = (1 - m_\mu^2/q^2)^2 [1 + m_\mu^2/(2q^2)]$. The formulas for the FFs $\mathcal{F}_{11,21,31}$ are given in Ref. [12]. The two-dimensional integration over $m_{\bar{K}^0\pi^-}^2$ and q^2 in Eq. (4) is constrained by the decay width $\Gamma[D^0 \rightarrow K^*(892)^-\mu^+\nu_\mu]$, which is derived by the measured $\mathcal{B}[D^0 \rightarrow K^*(892)^-\mu^+\nu_\mu]$ and the D^0 lifetime $\tau_{D^0} = 410.3 \pm 1.0$ fs [29]. We then obtain $A_1(0) = 0.623 \pm 0.008_{\text{stat}} \pm 0.008_{\text{syst}}$, which is measured for the first time using the decay $D^0 \rightarrow K^*(892)^-\mu^+\nu_\mu$.

In summary, with 7.9 fb^{-1} of e^+e^- annihilation data collected at $\sqrt{s} = 3.773$ GeV by the BESIII detector, the absolute BF of $D^0 \rightarrow \bar{K}^0\pi^-\mu^+\nu_\mu$ is measured for the first time to be $\mathcal{B}(D^0 \rightarrow \bar{K}^0\pi^-\mu^+\nu_\mu) = (1.373 \pm 0.020_{\text{stat}} \pm 0.023_{\text{syst}})\%$. By analyzing the dynamics of the $D^0 \rightarrow \bar{K}^0\pi^-\mu^+\nu_\mu$ decay, the \mathcal{S} -wave component is measured with a fraction $f_{\mathcal{S}\text{-wave}} = (5.35 \pm 0.87_{\text{stat}} \pm 0.71_{\text{syst}})\%$, leading to $\mathcal{B}[D^0 \rightarrow (\bar{K}^0\pi^-)_{\mathcal{S}\text{-wave}}\mu^+\nu_\mu] = (0.073 \pm 0.012_{\text{stat}} \pm 0.010_{\text{syst}})\%$. The \mathcal{P} -wave component is observed with a fraction of $f_{K^*(892)^-} = (94.60 \pm 0.87_{\text{stat}} \pm 0.71_{\text{syst}})\%$, and the corresponding BF is given as $\mathcal{B}[D^0 \rightarrow K^*(892)^-\mu^+\nu_\mu] = (1.948 \pm 0.033_{\text{stat}} \pm 0.036_{\text{syst}})\%$ with $\mathcal{B}[K^*(892)^- \rightarrow \bar{K}^0\pi^-] = 2/3$ under the assumption of the isospin symmetry. The FF ratios in the $D^0 \rightarrow K^*(892)^-\mu^+\nu_\mu$ decay are determined to be $r_V = 1.46 \pm 0.11_{\text{stat}} \pm 0.04_{\text{syst}}$ and $r_2 = 0.71 \pm 0.08_{\text{stat}} \pm 0.03_{\text{syst}}$. Meanwhile, using the FF parameters measured in this Letter, we also determine the ratio of partial widths for longitudinal and transverse K^* polarizations as defined in Refs. [24,33] to be $R_{L/T} = \Gamma_L/\Gamma_T = 1.21 \pm 0.05_{\text{stat+syst}}$, and the ratio of partial widths for positive and negative helicity defined in Ref. [24] to be $R_{+/-} = \Gamma_+/\Gamma_- = 0.28 \pm 0.03_{\text{stat+syst}}$ for the decay $D^0 \rightarrow K^*(892)^-\mu^+\nu_\mu$ for the first time. These results provide

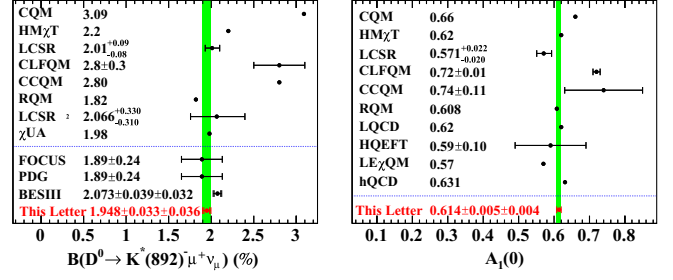


FIG. 3. Comparisons of the measured $\mathcal{B}[D^0 \rightarrow K^*(892)^-\mu^+\nu_\mu]$ and $A_1(0)$ with various theoretical calculations from the Lattice QCD [16], LCSR [17], LCSR 2 [18], CQM [19,20], HQEFT [21], HM χ T [22], CLFQM [23,24], LE χ QM [25], CCQM [26], RQM [27], hQCD [28], χ UA [34], and measurements from FOCUS [10], BESIII [13], and PDG averaged results [29].

important information in evaluating the pseudoscalar Wilson coefficient $c_P^{(\ell)}$ as in Ref. [33].

Averaging the results of r_V , r_2 and $A_1(0)$ reported previously in Refs. [12,13], we obtain the most precise measurements of FF parameters $r_V = 1.456 \pm 0.016_{\text{stat}} \pm 0.016_{\text{syst}}$, $r_2 = 0.715 \pm 0.031_{\text{stat}} \pm 0.014_{\text{stat}}$, and $A_1(0) = 0.614 \pm 0.005_{\text{stat}} \pm 0.004_{\text{syst}}$ in the $D^0 \rightarrow K^*(892)^-\mu^+\nu_\mu$ transition. The comparisons of the $\mathcal{B}[D^0 \rightarrow K^*(892)^-\mu^+\nu_\mu]$, $A_1(0)$, r_V , and r_2 between this measurement and theoretical calculations [16–28] are shown in Figs. 3 and 4. The central values calculated from the CQM [19,20], CLFQM [23,24], and CCQM [26] differ by more than two standard deviations with respect to the mean value of our measured BF. Thus, our measurement disfavors these predictions at a confidence level (CL) of more than 95%, while the measured r_V and r_2 in this Letter disfavor the central values calculated from the HM χ T [22], CLFQM [23,24], and RQM [27] by more than 3 standard deviations. Furthermore, using the $\mathcal{B}[D^0 \rightarrow K^*(892)^-e^+\nu_e]$ and $\mathcal{B}[D^0 \rightarrow \bar{K}^0\pi^-e^+\nu_e]$ measured in Ref. [12], we obtain the relative ratios between μ and e channels to be

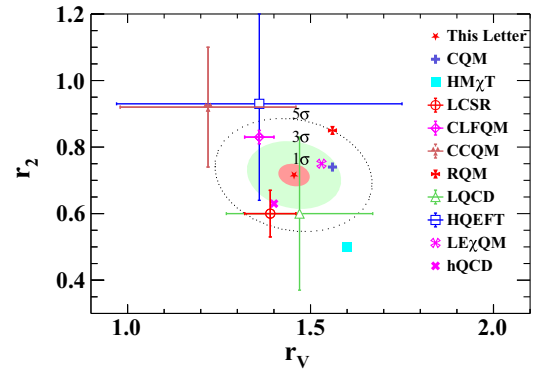


FIG. 4. Comparisons of the measured r_V and r_2 in this Letter with various theoretical calculations [16–28]. The correlation coefficient between the measured r_V and r_2 is -0.17 .

$$\mathcal{R}_{K^*(892)}^{\mu/e} = 0.955 \pm 0.022_{\text{stat}} \pm 0.017_{\text{syst}},$$

$$\begin{aligned} \mathcal{R}_{\bar{K}^0\pi}^{\mu/e} &= \frac{\mathcal{B}(D^0 \rightarrow \bar{K}^0\pi^-\mu^+\nu_\mu)}{\mathcal{B}(D^0 \rightarrow \bar{K}^0\pi^-e^+\nu_e)} \\ &= 0.951 \pm 0.020_{\text{stat}} \pm 0.016_{\text{syst}}. \end{aligned}$$

These ratios are in good agreement with the calculations in Refs. [17,20,24–27,34], but disfavor the calculation in Ref. [18] at 68% CL. The results presented in this Letter provide the most powerful tests and constraints on various theoretical calculations, especially in QCD theories, and play an important role in understanding the dynamics of SL decays of charmed hadrons in the nonperturbative region.

Acknowledgments—The BESIII Collaboration thanks the staff of BEPCII [46] and the IHEP computing center for their strong support. This work is supported in part by the National Key R&D Program of China under Contracts No. 2020YFA0406400, No. 2020YFA0406300, No. 2023YFA1606000, No. 2023YFA1606704; National Natural Science Foundation of China (NSFC) under Contracts No. 11635010, No. 11935015, No. 11935016, No. 11935018, No. 12022510, No. 12025502, No. 12035009, No. 12035013, No. 12061131003, No. 12192260, No. 12192261, No. 12192262, No. 12192263, No. 12192264, No. 12192265, No. 12221005, No. 12225509, No. 12235017, No. 12375090, No. 12475092, No. 12361141819; the Chinese Academy of Sciences (CAS) Large-Scale Scientific Facility Program; CAS under Contract No. YSBR-101; 100 Talents Program of CAS; The Institute of Nuclear and Particle Physics (INPAC) and Shanghai Key Laboratory for Particle Physics and Cosmology; Agencia Nacional de Investigación y Desarrollo de Chile (ANID), Chile under Contract No. ANID PIA/APOYO AFB230003; German Research Foundation DFG under Contract No. FOR5327; Istituto Nazionale di Fisica Nucleare, Italy; Knut and Alice Wallenberg Foundation under Contracts No. 2021.0174, No. 2021.0299; Ministry of Development of Turkey under Contract No. DPT2006K-120470; National Research Foundation of Korea under Contract No. NRF-2022R1A2C1092335; National Science and Technology fund of Mongolia; National Science Research and Innovation Fund (NSRF) via the Program Management Unit for Human Resources & Institutional Development, Research and Innovation of Thailand under Contract No. B50G670107; Polish National Science Centre under Contract No. 2024/53/B/ST2/00975; Swedish Research Council under Contract No. 2019.04595; U.S. Department of Energy under Contract No. DE-FG02-05ER41374. This paper is also supported by the Fundamental Research Funds for the Central

Universities, and the Research Funds of Renmin University of China under Contract No. 24XNKJ05.

Data availability—The data that support the findings of this Letter are not publicly available upon publication because it is not technically feasible and/or the cost of preparing, depositing, and hosting the data would be prohibitive within the terms of each research project. The data are available from the authors upon reasonable request.

-
- [1] M. Antonelli *et al.*, *Phys. Rep.* **494**, 197 (2010).
 - [2] J. D. Richman and P. R. Burchat, *Rev. Mod. Phys.* **67**, 893 (1995).
 - [3] N. Cabibbo, *Phys. Rev. Lett.* **10**, 531 (1963); M. Kobayashi and T. Maskawa, *Prog. Theor. Phys.* **49**, 652 (1973).
 - [4] M. Ablikim *et al.* (BESIII Collaboration), *Phys. Rev. Lett.* **122**, 061801 (2019).
 - [5] B. Aubert *et al.* (BABAR Collaboration), *Phys. Rev. D* **78**, 051101(R) (2008).
 - [6] M. R. Shepherd *et al.* (CLEO Collaboration), *Phys. Rev. D* **74**, 052001 (2006).
 - [7] R. A. Briere *et al.* (CLEO Collaboration), *Phys. Rev. D* **81**, 112001 (2006).
 - [8] P. del Amo Sanchez *et al.* (BABAR Collaboration), *Phys. Rev. D* **83**, 072001 (2011).
 - [9] M. Ablikim *et al.* (BESIII Collaboration), *Phys. Rev. D* **94**, 032001 (2016).
 - [10] J. M. Link *et al.* (FOCUS Collaboration), *Phys. Lett. B* **607**, 67 (2005).
 - [11] M. Ablikim *et al.* (BESIII Collaboration), *Phys. Rev. D* **99**, 011103(R) (2019).
 - [12] M. Ablikim *et al.* (BESIII Collaboration), *J. High Energy Phys.* **03** (2025) 197.
 - [13] M. Ablikim *et al.* (BESIII Collaboration), *Phys. Rev. Lett.* **134**, 011803 (2025).
 - [14] S. Dobbs *et al.* (CLEO Collaboration), *Phys. Rev. Lett.* **110**, 131802 (2013).
 - [15] M. Ablikim *et al.* (BESIII Collaboration), *Phys. Rev. D* **92**, 071101(R) (2015).
 - [16] A. Abada, D. Becirevic, Ph. Boucaud, J. M. Flynn, J. P. Lerory, V. Lubicz, and F. Mescia, *Nucl. Phys. B, Proc. Suppl.* **119**, 625 (2003).
 - [17] Y. L. Wu, M. Zhong, and Y. B. Zuo, *Int. J. Mod. Phys. A* **21**, 6125 (2006).
 - [18] H. B. Fu, W. Cheng, D. D. Hu, and T. Zhong, *Phys. Rev. Res.* **4**, 043129 (2022).
 - [19] D. Melikhov and B. Stech, *Phys. Rev. D* **62**, 014006 (2000).
 - [20] N. R. Soni and J. N. Pandya, *Phys. Rev. D* **96**, 016017 (2017).
 - [21] W. Y. Wang, Y. L. Wu, and M. Zhong, *Phys. Rev. D* **67**, 014024 (2003).
 - [22] S. Fajfer and J. Kamenik, *Phys. Rev. D* **72**, 034029 (2005).
 - [23] R. C. Verma, *J. Phys. G* **39**, 025005 (2012).
 - [24] H. Y. Cheng and X. W. Kang, *Eur. Phys. J. C* **77**, 587 (2017).
 - [25] T. Palmer and J. O. Eeg, *Phys. Rev. D* **89**, 034013 (2014).

- [26] M. A. Ivanov, J. G. Körner, J. N. Pandya, P. Santorelli, N. R. Soni, and C. T. Tran, *Front. Phys.* **14**, 64401 (2019).
- [27] R. N. Faustov, V. O. Galkin, and X. W. Kang, *Phys. Rev. D* **101**, 013004 (2020).
- [28] H. A. Ahmed, Y. D. Chen, and M. Huang, *Phys. Rev. D* **109**, 026008 (2024).
- [29] S. Navas *et al.* (Particle Data Group), *Phys. Rev. D* **110**, 030001 (2024).
- [30] B. C. Ke, J. Koponen, H. B. Li, and Y. H. Zheng, *Annu. Rev. Nucl. Part. Sci.* **73**, 285 (2023).
- [31] H. B. Li and X. R. Lyu, *Natl. Sci. Rev.* **8**, nwab181 (2021).
- [32] X. Leng, X. L. Mu, Z. T. Zou, and Y. Li, *Chin. Phys. C* **45**, 063107 (2021).
- [33] S. Fajfer, I. Nisandzic, and U. Rojec, *Phys. Rev. D* **91**, 094009 (2015).
- [34] T. Sekihara and E. Oset, *Phys. Rev. D* **92**, 054038 (2015).
- [35] M. Ablikim *et al.* (BESIII Collaboration), *Nucl. Instrum. Methods Phys. Res., Sect. A* **614**, 345 (2010).
- [36] S. Agostinelli *et al.* (GEANT4 Collaboration), *Nucl. Instrum. Methods Phys. Res., Sect. A* **506**, 250 (2003).
- [37] S. Jadach, B. F. L. Ward, and Z. Was, *Comput. Phys. Commun.* **130**, 260 (2000); *Phys. Rev. D* **63**, 113009 (2001).
- [38] D. J. Lange, *Nucl. Instrum. Methods Phys. Res., Sect. A* **462**, 152 (2001); R. G. Ping, *Chin. Phys. C* **32**, 599 (2008).
- [39] J. C. Chen, G. S. Huang, X. R. Qi, D. H. Zhang, and Y. S. Zhu, *Phys. Rev. D* **62**, 034003 (2000).
- [40] E. Richter-Was, *Phys. Lett. B* **303**, 163 (1993).
- [41] H. Albrecht *et al.* (ARGUS Collaboration), *Phys. Lett. B* **241**, 278 (1990).
- [42] The BF's of $K^0 \rightarrow K_S^0$ and $K_S^0 \rightarrow \pi^+\pi^-$ are not included in the detection efficiency. The K_S^0 fraction of K^0 is taken as 50%, and the BF of $K_S^0 \rightarrow \pi^+\pi^-$ is taken from PDG [29].
- [43] C. L. Y. Lee, M. Lu, and M. B. Wise, *Phys. Rev. D* **46**, 5040 (1992).
- [44] H. Zhang, B. C. Ke, Y. Yu, and E. Wang, *Chin. Phys. C* **47**, 063101 (2023).
- [45] See Supplemental Material at <http://link.aps.org/supplemental/10.1103/zfzfr-dlzg> for the detailed expression of the \mathcal{I} , and the systematic uncertainty for FF parameters.
- [46] <https://cstr.cn/31109.02.BEPC>

M. Ablikim,¹ M. N. Achasov,^{4,c} P. Adlarson,⁷⁷ X. C. Ai,⁸² R. Aliberti,³⁶ A. Amoroso,^{76a,76c} Q. An,^{73,59,a} Y. Bai,⁵⁸ O. Bakina,³⁷ Y. Ban,^{47,h} H.-R. Bao,⁶⁵ V. Batozskaya,^{1,45} K. Begzsuren,³³ N. Berger,³⁶ M. Berlowski,⁴⁵ M. Bertani,^{29a} D. Bettoni,^{30a} F. Bianchi,^{76a,76c} E. Bianco,^{76a,76c} A. Bortone,^{76a,76c} I. Boyko,³⁷ R. A. Briere,⁵ A. Brueggemann,⁷⁰ H. Cai,^{1,59} M. H. Cai,^{39,k,l} X. Cai,^{1,59} A. Calcaterra,^{29a} G. F. Cao,^{1,65} N. Cao,^{1,65} S. A. Cetin,^{63a} X. Y. Chai,^{47,h} J. F. Chang,^{1,59} G. R. Che,⁴⁴ Y. Z. Che,^{1,59,65} C. H. Chen,⁹ Chao Chen,⁵⁶ G. Chen,¹ H. S. Chen,^{1,65} H. Y. Chen,²¹ M. L. Chen,^{1,59,65} S. J. Chen,⁴³ S. L. Chen,⁴⁶ S. M. Chen,⁶² T. Chen,^{1,65} X. R. Chen,^{32,65} X. T. Chen,^{1,65} X. Y. Chen,^{12,g} Y. B. Chen,^{1,59} Y. Q. Chen,³⁵ Y. Q. Chen,¹⁶ Z. J. Chen,^{26,i} Z. K. Chen,⁶⁰ S. K. Choi,¹⁰ X. Chu,^{12,g} G. Cibinetto,^{30a} F. Cossio,^{76c} J. Cottee-Meldrum,⁶⁴ J. J. Cui,⁵¹ H. L. Dai,^{1,59} J. P. Dai,⁸⁰ A. Dbeyssi,¹⁹ R. E. de Boer,³ D. Dedovich,³⁷ C. Q. Deng,⁷⁴ Z. Y. Deng,¹ A. Denig,³⁶ I. Denysenko,³⁷ M. Destefanis,^{76a,76c} F. De Mori,^{76a,76c} B. Ding,^{68,1} X. X. Ding,^{47,h} Y. Ding,³⁵ Y. Ding,⁴¹ Y. Q. Ding,⁴⁹ Y. X. Ding,³¹ J. Dong,^{1,59} L. Y. Dong,^{1,65} M. Y. Dong,^{1,59,65} X. Dong,⁷⁸ M. C. Du,¹ S. X. Du,⁸² S. X. Du,^{12,g} Y. Y. Duan,⁵⁶ P. Egorov,^{37,b} G. F. Fan,⁴³ J. J. Fan,²⁰ Y. H. Fan,⁴⁶ J. Fang,⁶⁰ J. Fang,^{1,59} S. S. Fang,^{1,65} W. X. Fang,¹ Y. Q. Fang,^{1,59} R. Farinelli,^{30a} L. Fava,^{76b,76c} F. Feldbauer,³ G. Felici,^{29a} C. Q. Feng,^{73,59} J. H. Feng,¹⁶ L. Feng,^{39,k,l} Q. X. Feng,^{39,k,l} Y. T. Feng,^{73,59} M. Fritsch,³ C. D. Fu,¹ J. L. Fu,⁶⁵ Y. W. Fu,^{1,65} H. Gao,⁶⁵ X. B. Gao,⁴² Y. Gao,^{73,59} Y. N. Gao,^{47,h} Y. N. Gao,²⁰ Y. Y. Gao,³¹ S. Garbolino,^{76c} I. Garzia,^{30a,30b} P. T. Ge,²⁰ Z. W. Ge,⁴³ C. Geng,⁶⁰ E. M. Gersabeck,⁶⁹ A. Gilman,⁷¹ K. Goetzen,¹³ J. D. Gong,³⁵ L. Gong,⁴¹ W. X. Gong,^{1,59} W. Gradl,³⁶ S. Gramigna,^{30a,30b} M. Greco,^{76a,76c} M. H. Gu,^{1,59} Y. T. Gu,¹⁵ C. Y. Guan,^{1,65} A. Q. Guo,³² L. B. Guo,⁴² M. J. Guo,⁵¹ R. P. Guo,⁵⁰ Y. P. Guo,^{12,g} A. Guskov,^{37,b} J. Gutierrez,²⁸ K. L. Han,⁶⁵ T. T. Han,¹ F. Hanisch,³ K. D. Hao,^{73,59} X. Q. Hao,²⁰ F. A. Harris,⁶⁷ K. K. He,⁵⁶ K. L. He,^{1,65} F. H. Heinsius,³ C. H. Heinz,³⁶ Y. K. Heng,^{1,59,65} C. Herold,⁶¹ P. C. Hong,³⁵ G. Y. Hou,^{1,65} X. T. Hou,^{1,65} Y. R. Hou,⁶⁵ Z. L. Hou,¹ H. M. Hu,^{1,65} J. F. Hu,^{57,j} Q. P. Hu,^{73,59} S. L. Hu,^{12,g} T. Hu,^{1,59,65} Y. Hu,¹ Z. M. Hu,⁶⁰ G. S. Huang,^{73,59} K. X. Huang,⁶⁰ L. Q. Huang,^{32,65} P. Huang,⁴³ X. T. Huang,⁵¹ Y. P. Huang,¹ Y. S. Huang,⁶⁰ T. Hussain,⁷⁵ N. Hüsken,³⁶ N. in der Wiesche,⁷⁰ J. Jackson,²⁸ Q. Ji,¹ Q. P. Ji,²⁰ W. Ji,^{1,65} X. B. Ji,^{1,65} X. L. Ji,^{1,59} Y. Y. Ji,⁵¹ Z. K. Jia,^{73,59} D. Jiang,^{1,65} H. B. Jiang,⁷⁸ P. C. Jiang,^{47,h} S. J. Jiang,⁹ T. J. Jiang,¹⁷ X. S. Jiang,^{1,59,65} Y. Jiang,⁶⁵ J. B. Jiao,⁵¹ J. K. Jiao,³⁵ Z. Jiao,²⁴ S. Jin,⁴³ Y. Jin,⁶⁸ M. Q. Jing,^{1,65} X. M. Jing,⁶⁵ T. Johansson,⁷⁷ S. Kabana,³⁴ N. Kalantar-Nayestanaki,⁶⁶ X. L. Kang,⁹ X. S. Kang,⁴¹ M. Kavatsyuk,⁶⁶ B. C. Ke,⁸² V. Khachatryan,²⁸ A. Khoukaz,⁷⁰ R. Kiuchi,¹ O. B. Kolcu,^{63a} B. Kopf,³ M. Kuessner,³ X. Kui,^{1,65} N. Kumar,²⁷ A. Kupsc,^{45,77} W. Kühn,³⁸ Q. Lan,⁷⁴ W. N. Lan,²⁰ T. T. Lei,^{73,59} M. Lellmann,³⁶ T. Lenz,³⁶ C. Li,⁴⁸ C. Li,^{73,59} C. Li,⁴⁴ C. H. Li,⁴⁰ C. K. Li,²¹ D. M. Li,⁸² F. Li,^{1,59} G. Li,¹ H. B. Li,^{1,65} H. J. Li,²⁰ H. N. Li,^{57,j} Hui Li,⁴⁴ J. R. Li,⁶² J. S. Li,⁶⁰ K. Li,¹ K. L. Li,²⁰ K. L. Li,^{39,k,l} L. J. Li,^{1,65} Lei Li,⁴⁹ M. H. Li,⁴⁴ M. R. Li,^{1,65} P. L. Li,⁶⁵ P. R. Li,^{39,k,l} Q. M. Li,^{1,65} Q. X. Li,⁵¹ R. Li,^{18,32} S. X. Li,¹² T. Li,⁵¹ T. Y. Li,⁴⁴ W. D. Li,^{1,65} W. G. Li,^{1,a}

X. Li,^{1,65} X. H. Li,^{73,59} X. L. Li,⁵¹ X. Y. Li,^{1,8} X. Z. Li,⁶⁰ Y. Li,²⁰ Y. G. Li,^{47,h} Y. P. Li,³⁵ Z. J. Li,⁶⁰ Z. Y. Li,⁸⁰ H. Liang,^{73,59} Y. F. Liang,⁵⁵ Y. T. Liang,^{32,65} G. R. Liao,¹⁴ L. B. Liao,⁶⁰ M. H. Liao,⁶⁰ Y. P. Liao,^{1,65} J. Libby,²⁷ A. Limphirat,⁶¹ C. C. Lin,⁵⁶ D. X. Lin,^{32,65} L. Q. Lin,⁴⁰ T. Lin,¹ B. J. Liu,¹ B. X. Liu,⁷⁸ C. Liu,³⁵ C. X. Liu,¹ F. Liu,¹ F. H. Liu,⁵⁴ Feng Liu,⁶ G. M. Liu,^{57,j} H. Liu,^{39,k,l} H. B. Liu,¹⁵ H. H. Liu,¹ H. M. Liu,^{1,65} Huihui Liu,²² J. B. Liu,^{73,59} J. J. Liu,²¹ K. Liu,^{39,k,l} K. Liu,⁷⁴ K. Y. Liu,⁴¹ Ke Liu,²³ L. C. Liu,⁴⁴ Lu Liu,⁴⁴ M. H. Liu,^{12,g} P. L. Liu,¹ Q. Liu,⁶⁵ S. B. Liu,^{73,59} T. Liu,^{12,g} W. K. Liu,⁴⁴ W. M. Liu,^{73,59} W. T. Liu,⁴⁰ X. Liu,^{39,k,l} X. Liu,⁴⁰ X. K. Liu,^{39,k,l} X. Y. Liu,⁷⁸ Y. Liu,⁸² Y. Liu,^{39,k,l} Y. Liu,⁸² Y. B. Liu,⁴⁴ Z. A. Liu,^{1,59,65} Z. D. Liu,⁹ Z. Q. Liu,⁵¹ X. C. Lou,^{1,59,65} F. X. Lu,⁶⁰ H. J. Lu,²⁴ J. G. Lu,^{1,59} X. L. Lu,¹⁶ Y. Lu,⁷ Y. H. Lu,^{1,65} Y. P. Lu,^{1,59} Z. H. Lu,^{1,65} C. L. Luo,⁴² J. R. Luo,⁶⁰ J. S. Luo,^{1,65} M. X. Luo,⁸¹ T. Luo,^{12,g} X. L. Luo,^{1,59} Z. Y. Lv,²³ X. R. Lyu,^{65,p} Y. F. Lyu,⁴⁴ Y. H. Lyu,⁸² F. C. Ma,⁴¹ H. Ma,²⁶ H. L. Ma,¹ J. L. Ma,^{1,65} L. L. Ma,⁵¹ L. R. Ma,⁶⁸ Q. M. Ma,¹ R. Q. Ma,^{1,65} R. Y. Ma,²⁰ T. Ma,^{73,59} X. T. Ma,^{1,65} X. Y. Ma,^{1,59} Y. M. Ma,³² F. E. Maas,¹⁹ I. MacKay,⁷¹ M. Maggiora,^{76a,76c} S. Malde,⁷¹ Q. A. Malik,⁷⁵ H. X. Mao,^{39,k,l} Y. J. Mao,^{47,h} Z. P. Mao,¹ S. Marcello,^{76a,76c} A. Marshall,⁶⁴ F. M. Melendi,^{30a,30b} Y. H. Meng,⁶⁵ Z. X. Meng,⁶⁸ G. Mezzadri,^{30a} H. Miao,^{1,65} T. J. Min,⁴³ R. E. Mitchell,²⁸ X. H. Mo,^{1,59,65} B. Moses,²⁸ N. Yu. Muchnoi,^{4,c} J. Muskalla,³⁶ Y. Nefedov,³⁷ F. Nerling,^{19,e} L. S. Nie,²¹ I. B. Nikolaev,^{4,c} Z. Ning,^{1,59} S. Nisar,^{11,m} Q. L. Niu,^{39,k,l} W. D. Niu,^{12,g} C. Normand,⁶⁴ S. L. Olsen,^{10,65} Q. Ouyang,^{1,59,65} S. Pacetti,^{29b,29c} X. Pan,⁵⁶ Y. Pan,⁵⁸ A. Pathak,¹⁰ Y. P. Pei,^{73,59} M. Pelizaeus,³ H. P. Peng,^{73,59} X. J. Peng,^{39,k,l} Y. Y. Peng,^{39,k,l} K. Peters,^{13,e} K. Petridis,⁶⁴ J. L. Ping,⁴² R. G. Ping,^{1,65} S. Plura,³⁶ V. Prasad,³⁵ F. Z. Qi,¹ H. R. Qi,⁶² M. Qi,⁴³ S. Qian,^{1,59} W. B. Qian,⁶⁵ C. F. Qiao,⁶⁵ J. H. Qiao,²⁰ J. J. Qin,⁷⁴ J. L. Qin,⁵⁶ L. Q. Qin,¹⁴ L. Y. Qin,^{73,59} P. B. Qin,⁷⁴ X. P. Qin,^{12,g} X. S. Qin,⁵¹ Z. H. Qin,^{1,59} J. F. Qiu,¹ Z. H. Qu,⁷⁴ J. Rademacker,⁶⁴ C. F. Redmer,³⁶ A. Rivetti,^{76c} M. Rolo,^{76c} G. Rong,^{1,65} S. S. Rong,^{1,65} F. Rosini,^{29b,29c} Ch. Rosner,¹⁹ M. Q. Ruan,^{1,59} N. Salone,⁴⁵ A. Sarantsev,^{37,d} Y. Schelhaas,³⁶ K. Schoenning,⁷⁷ M. Scodreggio,^{30a} K. Y. Shan,^{12,g} W. Shan,²⁵ X. Y. Shan,^{73,59} Z. J. Shang,^{39,k,l} J. F. Shangguan,¹⁷ L. G. Shao,^{1,65} M. Shao,^{73,59} C. P. Shen,^{12,g} H. F. Shen,^{1,8} W. H. Shen,⁶⁵ X. Y. Shen,^{1,65} B. A. Shi,⁶⁵ H. Shi,^{73,59} J. L. Shi,^{12,g} J. Y. Shi,¹ S. Y. Shi,⁷⁴ X. Shi,^{1,59} H. L. Song,^{73,59} J. J. Song,²⁰ T. Z. Song,⁶⁰ W. M. Song,³⁵ Y. J. Song,^{12,g} Y. X. Song,^{47,h,n} S. Sosio,^{76a,76c} S. Spataro,^{76a,76c} F. Stieler,³⁶ S. S. Su,⁴¹ Y. J. Su,⁶⁵ G. B. Sun,⁷⁸ G. X. Sun,¹ H. Sun,⁶⁵ H. K. Sun,¹ J. F. Sun,²⁰ K. Sun,⁶² L. Sun,⁷⁸ S. S. Sun,^{1,65} T. Sun,^{52,f} Y. C. Sun,⁷⁸ Y. H. Sun,³¹ Y. J. Sun,^{73,59} Y. Z. Sun,¹ Z. Q. Sun,^{1,65} Z. T. Sun,⁵¹ C. J. Tang,⁵⁵ G. Y. Tang,¹ J. Tang,⁶⁰ J. J. Tang,^{73,59} L. F. Tang,⁴⁰ Y. A. Tang,⁷⁸ L. Y. Tao,⁷⁴ M. Tat,⁷¹ J. X. Teng,^{73,59} J. Y. Tian,^{73,59} W. H. Tian,⁶⁰ Y. Tian,³² Z. F. Tian,⁷⁸ I. Uman,^{63b} B. Wang,⁶⁰ B. Wang,¹ Bo Wang,^{73,59} C. Wang,^{39,k,l} C. Wang,²⁰ Cong Wang,²³ D. Y. Wang,^{47,h} H. J. Wang,^{39,k,l} J. J. Wang,⁷⁸ K. Wang,^{1,59} L. L. Wang,¹ L. W. Wang,³⁵ M. Wang,^{73,59} M. Wang,⁵¹ N. Y. Wang,⁶⁵ S. Wang,^{12,g} T. Wang,^{12,g} T. J. Wang,⁴⁴ W. Wang,⁶⁰ W. Wang,⁷⁴ W. P. Wang,^{36,59,73,o} X. Wang,^{47,h} X. F. Wang,^{39,k,l} X. J. Wang,⁴⁰ X. L. Wang,^{12,g} X. N. Wang,¹ Y. Wang,⁶² Y. D. Wang,⁴⁶ Y. F. Wang,^{1,8,65} Y. H. Wang,^{39,k,l} Y. J. Wang,^{73,59} Y. L. Wang,²⁰ Y. N. Wang,⁷⁸ Y. Q. Wang,¹ Yaqian Wang,¹⁸ Yi Wang,⁶² Yuan Wang,^{18,32} Z. Wang,^{1,59} Z. L. Wang,² Z. L. Wang,⁷⁴ Z. Q. Wang,^{12,g} Z. Y. Wang,^{1,65} D. H. Wei,¹⁴ H. R. Wei,⁴⁴ F. Weidner,⁷⁰ S. P. Wen,¹ Y. R. Wen,⁴⁰ U. Wiedner,³ G. Wilkinson,⁷¹ M. Wolke,⁷⁷ C. Wu,⁴⁰ J. F. Wu,^{1,8} L. H. Wu,¹ L. J. Wu,^{1,65} L. J. Wu,²⁰ Lianjie Wu,²⁰ S. G. Wu,^{1,65} S. M. Wu,⁶⁵ X. Wu,^{12,g} X. H. Wu,³⁵ Y. J. Wu,³² Z. Wu,^{1,59} L. Xia,^{73,59} X. M. Xian,⁴⁰ B. H. Xiang,^{1,65} D. Xiao,^{39,k,l} G. Y. Xiao,⁴³ H. Xiao,⁷⁴ Y. L. Xiao,^{12,g} Z. J. Xiao,⁴² C. Xie,⁴³ K. J. Xie,^{1,65} X. H. Xie,^{47,h} Y. Xie,⁵¹ Y. G. Xie,^{1,59} Y. H. Xie,⁶ Z. P. Xie,^{73,59} T. Y. Xing,^{1,65} C. F. Xu,^{1,65} C. J. Xu,⁶⁰ G. F. Xu,¹ H. Y. Xu,^{68,2} H. Y. Xu,² M. Xu,^{73,59} Q. J. Xu,¹⁷ Q. N. Xu,³¹ T. D. Xu,⁷⁴ W. Xu,¹ W. L. Xu,⁶⁸ X. P. Xu,⁵⁶ Y. Xu,⁴¹ Y. Xu,^{12,g} Y. C. Xu,⁷⁹ Z. S. Xu,⁶⁵ F. Yan,^{12,g} H. Y. Yan,⁴⁰ L. Yan,^{12,g} W. B. Yan,^{73,59} W. C. Yan,⁸² W. H. Yan,⁶ W. P. Yan,²⁰ X. Q. Yan,^{1,65} H. J. Yang,^{52,f} H. L. Yang,³⁵ H. X. Yang,¹ J. H. Yang,⁴³ R. J. Yang,²⁰ T. Yang,¹ Y. Yang,^{12,g} Y. F. Yang,⁴⁴ Y. H. Yang,⁴³ Y. Q. Yang,⁹ Y. X. Yang,^{1,65} Y. Z. Yang,²⁰ M. Ye,^{1,59} M. H. Ye,^{8,a} Z. J. Ye,^{57,j} Junhao Yin,⁴⁴ Z. Y. You,⁶⁰ B. X. Yu,^{1,59,65} C. X. Yu,⁴⁴ G. Yu,¹³ J. S. Yu,^{26,i} L. Q. Yu,^{12,g} M. C. Yu,⁴¹ T. Yu,⁷⁴ X. D. Yu,^{47,h} Y. C. Yu,⁸² C. Z. Yuan,^{1,65} H. Yuan,^{1,65} J. Yuan,³⁵ J. Yuan,⁴⁶ L. Yuan,² S. C. Yuan,^{1,65} X. Q. Yuan,¹ Y. Yuan,^{1,65} Z. Y. Yuan,⁶⁰ C. X. Yue,⁴⁰ Ying Yue,²⁰ A. A. Zafar,⁷⁵ S. H. Zeng,⁶⁴ X. Zeng,^{12,g} Y. Zeng,^{26,i} Y. J. Zeng,⁶⁰ Y. J. Zeng,^{1,65} X. Y. Zhai,³⁵ Y. H. Zhan,⁶⁰ A. Q. Zhang,^{1,65} B. L. Zhang,^{1,65} B. X. Zhang,¹ D. H. Zhang,⁴⁴ G. Y. Zhang,^{1,65} G. Y. Zhang,²⁰ H. Zhang,^{73,59} H. Zhang,⁸² H. C. Zhang,^{1,59,65} H. H. Zhang,⁶⁰ H. Q. Zhang,^{1,59,65} H. R. Zhang,^{73,59} H. Y. Zhang,^{1,59} J. Zhang,⁶⁰ J. Zhang,⁸² J. J. Zhang,⁵³ J. L. Zhang,²¹ J. Q. Zhang,⁴² J. S. Zhang,^{12,g} J. W. Zhang,^{1,59,65} J. X. Zhang,^{39,k,l} J. Y. Zhang,¹ J. Z. Zhang,^{1,65} Jianyu Zhang,⁶⁵ L. M. Zhang,⁶² Lei Zhang,⁴³ N. Zhang,⁸² P. Zhang,^{1,8} Q. Zhang,²⁰ Q. Y. Zhang,³⁵ R. Y. Zhang,^{39,k,l} S. H. Zhang,^{1,65} Shulei Zhang,^{26,i} X. M. Zhang,¹ X. Y. Zhang,⁴¹ X. Y. Zhang,⁵¹ Y. Zhang,⁷⁴ Y. Zhang,¹ Y. T. Zhang,⁸² Y. H. Zhang,^{1,59} Y. M. Zhang,⁴⁰ Y. P. Zhang,^{73,59} Z. D. Zhang,¹ Z. H. Zhang,¹ Z. L. Zhang,³⁵ Z. L. Zhang,⁵⁶ Z. X. Zhang,²⁰ Z. Y. Zhang,⁷⁸ Z. Y. Zhang,⁴⁴ Z. Z. Zhang,⁴⁶ Zh. Zh. Zhang,²⁰ G. Zhao,¹ J. Y. Zhao,^{1,65} J. Z. Zhao,^{1,59} L. Zhao,^{73,59} L. Zhao,¹ M. G. Zhao,⁴⁴ N. Zhao,⁸⁰ R. P. Zhao,⁶⁵ S. J. Zhao,⁸² Y. B. Zhao,^{1,59}

Y. L. Zhao,⁵⁶ Y. X. Zhao,^{32,65} Z. G. Zhao,^{73,59} A. Zhemchugov,^{37,b} B. Zheng,⁷⁴ B. M. Zheng,³⁵ J. P. Zheng,^{1,59}
 W. J. Zheng,^{1,65} X. R. Zheng,²⁰ Y. H. Zheng,^{65,p} B. Zhong,⁴² C. Zhong,²⁰ H. Zhou,^{36,51,o} J. Q. Zhou,³⁵ J. Y. Zhou,³⁵ S. Zhou,⁶
 X. Zhou,⁷⁸ X. K. Zhou,⁶ X. R. Zhou,^{73,59} X. Y. Zhou,⁴⁰ Y. X. Zhou,⁷⁹ Y. Z. Zhou,^{12,g} A. N. Zhu,⁶⁵ J. Zhu,⁴⁴ K. Zhu,¹
 K. J. Zhu,^{1,59,65} K. S. Zhu,^{12,g} L. Zhu,³⁵ L. X. Zhu,⁶⁵ S. H. Zhu,⁷² T. J. Zhu,^{12,g} W. D. Zhu,^{12,g} W. D. Zhu,⁴² W. J. Zhu,¹
 W. Z. Zhu,²⁰ Y. C. Zhu,^{73,59} Z. A. Zhu,^{1,65} X. Y. Zhuang,⁴⁴ J. H. Zou,¹ and J. Zu^{73,59}

(BESIII Collaboration)

- ¹*Institute of High Energy Physics, Beijing 100049, People's Republic of China*
²*Beihang University, Beijing 100191, People's Republic of China*
³*Bochum Ruhr-University, D-44780 Bochum, Germany*
⁴*Budker Institute of Nuclear Physics SB RAS (BINP), Novosibirsk 630090, Russia*
⁵*Carnegie Mellon University, Pittsburgh, Pennsylvania 15213, USA*
⁶*Central China Normal University, Wuhan 430079, People's Republic of China*
⁷*Central South University, Changsha 410083, People's Republic of China*
⁸*China Center of Advanced Science and Technology, Beijing 100190, People's Republic of China*
⁹*China University of Geosciences, Wuhan 430074, People's Republic of China*
¹⁰*Chung-Ang University, Seoul, 06974, Republic of Korea*
¹¹*COMSATS University Islamabad, Lahore Campus, Defence Road, Off Raiwind Road, 54000 Lahore, Pakistan*
¹²*Fudan University, Shanghai 200433, People's Republic of China*
¹³*GSI Helmholtzcentre for Heavy Ion Research GmbH, D-64291 Darmstadt, Germany*
¹⁴*Guangxi Normal University, Guilin 541004, People's Republic of China*
¹⁵*Guangxi University, Nanning 530004, People's Republic of China*
¹⁶*Guangxi University of Science and Technology, Liuzhou 545006, People's Republic of China*
¹⁷*Hangzhou Normal University, Hangzhou 310036, People's Republic of China*
¹⁸*Hebei University, Baoding 071002, People's Republic of China*
¹⁹*Helmholtz Institute Mainz, Staudinger Weg 18, D-55099 Mainz, Germany*
²⁰*Henan Normal University, Xinxiang 453007, People's Republic of China*
²¹*Henan University, Kaifeng 475004, People's Republic of China*
²²*Henan University of Science and Technology, Luoyang 471003, People's Republic of China*
²³*Henan University of Technology, Zhengzhou 450001, People's Republic of China*
²⁴*Huangshan College, Huangshan 245000, People's Republic of China*
²⁵*Hunan Normal University, Changsha 410081, People's Republic of China*
²⁶*Hunan University, Changsha 410082, People's Republic of China*
²⁷*Indian Institute of Technology Madras, Chennai 600036, India*
²⁸*Indiana University, Bloomington, Indiana 47405, USA*
^{29a}*INFN Laboratori Nazionali di Frascati, I-00044, Frascati, Italy*
^{29b}*INFN Sezione di Perugia, I-06100, Perugia, Italy*
^{29c}*University of Perugia, I-06100, Perugia, Italy*
^{30a}*INFN Sezione di Ferrara, I-44122, Ferrara, Italy*
^{30b}*University of Ferrara, I-44122, Ferrara, Italy*
³¹*Inner Mongolia University, Hohhot 010021, People's Republic of China*
³²*Institute of Modern Physics, Lanzhou 730000, People's Republic of China*
³³*Institute of Physics and Technology, Mongolian Academy of Sciences, Peace Avenue 54B, Ulaanbaatar 13330, Mongolia*
³⁴*Instituto de Alta Investigación, Universidad de Tarapacá, Casilla 7D, Arica 1000000, Chile*
³⁵*Jilin University, Changchun 130012, People's Republic of China*
³⁶*Johannes Gutenberg University of Mainz, Johann-Joachim-Becher-Weg 45, D-55099 Mainz, Germany*
³⁷*Joint Institute for Nuclear Research, 141980 Dubna, Moscow region, Russia*
³⁸*Justus-Liebig-Universität Giessen, II. Physikalisches Institut, Heinrich-Buff-Ring 16, D-35392 Giessen, Germany*
³⁹*Lanzhou University, Lanzhou 730000, People's Republic of China*
⁴⁰*Liaoning Normal University, Dalian 116029, People's Republic of China*
⁴¹*Liaoning University, Shenyang 110036, People's Republic of China*
⁴²*Nanjing Normal University, Nanjing 210023, People's Republic of China*
⁴³*Nanjing University, Nanjing 210093, People's Republic of China*
⁴⁴*Nankai University, Tianjin 300071, People's Republic of China*
⁴⁵*National Centre for Nuclear Research, Warsaw 02-093, Poland*
⁴⁶*North China Electric Power University, Beijing 102206, People's Republic of China*

- ⁴⁷*Peking University, Beijing 100871, People's Republic of China*
⁴⁸*Qufu Normal University, Qufu 273165, People's Republic of China*
⁴⁹*Renmin University of China, Beijing 100872, People's Republic of China*
⁵⁰*Shandong Normal University, Jinan 250014, People's Republic of China*
⁵¹*Shandong University, Jinan 250100, People's Republic of China*
⁵²*Shanghai Jiao Tong University, Shanghai 200240, People's Republic of China*
⁵³*Shanxi Normal University, Linfen 041004, People's Republic of China*
⁵⁴*Shanxi University, Taiyuan 030006, People's Republic of China*
⁵⁵*Sichuan University, Chengdu 610064, People's Republic of China*
⁵⁶*Soochow University, Suzhou 215006, People's Republic of China*
⁵⁷*South China Normal University, Guangzhou 510006, People's Republic of China*
⁵⁸*Southeast University, Nanjing 211100, People's Republic of China*
⁵⁹*State Key Laboratory of Particle Detection and Electronics, Beijing 100049, Hefei 230026, People's Republic of China*
⁶⁰*Sun Yat-Sen University, Guangzhou 510275, People's Republic of China*
⁶¹*Suranaree University of Technology, University Avenue 111, Nakhon Ratchasima 30000, Thailand*
⁶²*Tsinghua University, Beijing 100084, People's Republic of China*
^{63a}*Turkish Accelerator Center Particle Factory Group, Istinye University, 34010, Istanbul, Turkey*
^{63b}*Near East University, Nicosia, North Cyprus, 99138, Mersin 10, Turkey*
⁶⁴*University of Bristol, H H Wills Physics Laboratory, Tyndall Avenue, Bristol, BS8 1TL, United Kingdom*
⁶⁵*University of Chinese Academy of Sciences, Beijing 100049, People's Republic of China*
⁶⁶*University of Groningen, NL-9747 AA Groningen, The Netherlands*
⁶⁷*University of Hawaii, Honolulu, Hawaii 96822, USA*
⁶⁸*University of Jinan, Jinan 250022, People's Republic of China*
⁶⁹*University of Manchester, Oxford Road, Manchester, M13 9PL, United Kingdom*
⁷⁰*University of Muenster, Wilhelm-Klemm-Strasse 9, 48149 Muenster, Germany*
⁷¹*University of Oxford, Keble Road, Oxford OX13RH, United Kingdom*
⁷²*University of Science and Technology Liaoning, Anshan 114051, People's Republic of China*
⁷³*University of Science and Technology of China, Hefei 230026, People's Republic of China*
⁷⁴*University of South China, Hengyang 421001, People's Republic of China*
⁷⁵*University of the Punjab, Lahore-54590, Pakistan*
^{76a}*University of Turin and INFN, University of Turin, I-10125, Turin, Italy*
^{76b}*University of Eastern Piedmont, I-15121, Alessandria, Italy*
^{76c}*INFN, I-10125, Turin, Italy*
⁷⁷*Uppsala University, Box 516, SE-75120 Uppsala, Sweden*
⁷⁸*Wuhan University, Wuhan 430072, People's Republic of China*
⁷⁹*Yantai University, Yantai 264005, People's Republic of China*
⁸⁰*Yunnan University, Kunming 650500, People's Republic of China*
⁸¹*Zhejiang University, Hangzhou 310027, People's Republic of China*
⁸²*Zhengzhou University, Zhengzhou 450001, People's Republic of China*

^aDeceased.

^bAlso at the Moscow Institute of Physics and Technology, Moscow 141700, Russia.

^cAlso at the Novosibirsk State University, Novosibirsk, 630090, Russia.

^dAlso at the NRC "Kurchatov Institute," PNPI, 188300, Gatchina, Russia.

^eAlso at Goethe University Frankfurt, 60323 Frankfurt am Main, Germany.

^fAlso at Key Laboratory for Particle Physics, Astrophysics and Cosmology, Ministry of Education; Shanghai Key Laboratory for Particle Physics and Cosmology; Institute of Nuclear and Particle Physics, Shanghai 200240, People's Republic of China.

^gAlso at Key Laboratory of Nuclear Physics and Ion-beam Application (MOE) and Institute of Modern Physics, Fudan University, Shanghai 200443, People's Republic of China.

^hAlso at State Key Laboratory of Nuclear Physics and Technology, Peking University, Beijing 100871, People's Republic of China.

ⁱAlso at School of Physics and Electronics, Hunan University, Changsha 410082, China.

^jAlso at Guangdong Provincial Key Laboratory of Nuclear Science, Institute of Quantum Matter, South China Normal University, Guangzhou 510006, China.

^kAlso at MOE Frontiers Science Center for Rare Isotopes, Lanzhou University, Lanzhou 730000, People's Republic of China.

^lAlso at Lanzhou Center for Theoretical Physics, Lanzhou University, Lanzhou 730000, People's Republic of China.

^mAlso at the Department of Mathematical Sciences, IBA, Karachi 75270, Pakistan.

ⁿAlso at Ecole Polytechnique Federale de Lausanne (EPFL), CH-1015 Lausanne, Switzerland.

^oAlso at Helmholtz Institute Mainz, Staudinger Weg 18, D-55099 Mainz, Germany.

^pAlso at Hangzhou Institute for Advanced Study, University of Chinese Academy of Sciences, Hangzhou 310024, China.